International Journal of Applied Mathematics and Theoretical Physics
2025, Vol. 11, No. 4, pp. 49-68
https://doi.org/10.11648/j.ijamtp.20251104.11

Research Article

Performance of a Horizontal Well in an Anisotropic Oil Reservoir Subject to Simultaneous Double Edge Water Drive Mechanisms at Late Time Flow Regime

Mutili Peter Mutisya*

Department of Mathematics and Actuarial Science, Kenyatta University, Nairobi, Kenya

Abstract

Pressure distribution in horizontal wells mostly involves solving the diffusivity equation. Mathematical models take into account factors like permeability anisotropy, reservoir geometry and wellbore characteristics. The models use concepts like source and Green's functions to approximate pressure behavior particularly during various flow regimes like early radial, early linear, late pseudo radial and late linear. Mostly models consider the effects of boundaries like edge and bottom water drives and well completion strategies on pressure distribution. In this study reservoir characterization and description of the reservoir system form ways of actualizing prolonged clean oil production which is fundamental in all aspects of reservoir and petroleum engineering based on dimensionless pressure and dimensionless pressure derivative distribution in horizontal wells in oil reservoirs with water drive mechanisms. MATLAB programming was deployed in solving complex models and generating pressure and pressure derivative distribution plots. Since discrete data was used, cubic spline interpolation technique was used in generating smooth curves log – log plots. The results of the study show, at dimensionless breakthrough time (t_{DBr}), the dimensionless pressure derivative collapses to zero when dimensionless pressure exhibits a constant trend. In addition, t_{DBr} varies as $h_D y_{eD}/L_D$ and the dimensionless pressure varies directly as x^2_{eD} and inversely as y_{eD}, P_D varies as x^2_{eD} / y_{eD}. Further from this study, $x_D = x_{wD}$, $y_{eD} = 2y_D = 2y_{wD}$ and $z_{eD} = h_D = 2z_{wD}$ and prolonged L_D mar clean oil production. The information presented in this paper will assist the reservoir and petroleum engineers in designing correctly the horizontal well in the oil reservoir in order to enhance prolonged clean oil production.

Keywords

Horizontal Well, Reservoir, Double Edge, Water Drive, Late Time Flow

1. Introduction

The Source and Green's functions was first developed by Gringarten A. C. and Ramey H. J. [1]. The methods used in solving diffusivity equation in fluid flow are exponential integral solution and the dimensionless pressure solution. In this study dimensionless pressure and dimensionless pressure derivative solution was deployed together with the Newman product rule to perform a well test analysis of a horizontal well in an anisotropic oil reservoir at late time linear flow regime subject to simultaneous double edge water drive mechanisms. Mathematical tools and techniques used include

*Corresponding author: petermutili@gmail.com (Mutili Peter Mutisya)

Received: 1 September 2025; **Accepted:** 16 September 2025; **Published:** 9 October 2025

diffusivity equation which describes flow of a fluid in a porous media forming basis for pressure distribution. Source and Green's functions are tools we use to solve the diffusivity equation for reservoirs and horizontal well configurations. Dimensionless variables simplify the equations by use of parameters like dimensionless pressure and dimensionless time which allow more general analysis and efficient comparison of results.

Mathematical models are usually important in interpreting well test data and determination of properties of reservoirs like permeability and skin factor. Comprehending pressure distribution in oil reservoirs, is usually of great help to reservoir and petroleum engineers in optimizing well placement, production rates and well completion strategies. In addition, models assist in characterizing reservoir geometry, boundary types and permeability distribution in oil and gas reservoirs. Efficient use of mathematical models, reservoir and petroleum engineers can enhance the understanding and prediction of pressure behaviour in horizontal wells with the prime idea of efficient and profitable clean oil and gas production in our oil industry. Adewole E. S. studied procedures for analyzing interference tests data to determine the degree of communication between points in a reservoir system utilizing source and Green's functions in deriving appropriate dimensionless pressure expressions for a reservoir, bounded laterally by double-edged water drive mechanism consisting of horizontal and vertical well combinations [2]. As a late time flow test, they considered external distances between the wells in the computation of dimensionless pressure derivatives from the dimensionless pressure expressions derived. They also derived analytical expressions for analyzing interference test data for each well combination. The results show that, if the reservoir is isotropic, interference test duration should be less than water breakthrough time $t_{Dbr} \geq x_{eD}^2/\pi^2$ for valid results. Flow time beyond this limit gives only an indication of the strength and responsiveness of the encroaching aquifer. Horizontal well combinations would produce earlier interference than vertical-vertical well combinations, given the same anisotropy and rate history. Time of occurrence of interference is directly proportional to area between interfering wells.

Henry Idudje and Steve Adewole realized that, for very old wells and tight reservoirs it would take painfully long shut-in time to eventually attain the initial reservoir pressure before drawdown while in largely depleted reservoirs, it may be impossible to actually attain the desired initial reservoir pressure even after a long shut-in [3]. In their study they developed a procedure to overcome these challenges. They employed mathematical procedures based on selection of relevant source and Green's functions for a horizontal well during infinite-acting flow and assuming purely the well is a line source. Their results were analyzed on a semi log plot of flowing wellbore pressures versus time. The plots gave a straight line with intercept on the flowing wellbore pressure axis yielding the remaining reservoir pressure on extrapolation to dimensionless pressure of zero. Malekzadeh D. and Tiab D. solved the problem of interference testing of horizontal wells as a major step forward in understanding the fluid flow behavior of horizontal wells towards efficient implementation of the horizontal well technology [4]. They induced, these tests provide valuable information about reservoir characteristics such as storage, real average transmissibility and degree of communication between wells. Their study provided the dimensionless pressure and dimensionless pressure derivative type curves for interference testing of horizontal wells and the appropriate equations to be used in conjunction with the type curves in order to determine transmissibility and storage from field data. Their results suggested that the transmissibility and storage obtained from interference testing of horizontal wells would be much more representative of the formation than the ones obtained from interference testing of vertical wells. They also recommended that the determination of dimensionless pressure at the horizontal wellbore requires calculating the P_D function at small values of both y_D and z_D.

Emumena E., Adewole E.S. and Ojah M.G. utilized the solution to the dimensionless diffusivity equation using Laplace transform and modified Bessel equation in deriving a solution to the problem of interference testing of an active horizontal well in the presence of an active vertical well located in an infinite acting isotropic reservoir [5]. Their work investigates the effects of separation distance between active and observation wells, well lengths and wellbore radius on the pressure response at the observation well and the influence of the number of active wells, Locations and timing of activities of active wells on the pressure response at the observation well. Results from their study showed that larger magnitudes of dimensionless pressure and derivative would indicate higher oil production for any well design. Ojah M.G., Adewole E.S. and Emumena E. presented an accurate method for evaluating the performance of both the vertical and horizontal wells each located within an intersecting sealing or no-flow boundary and a constant-pressure boundary [6]. They investigated the transient pressure behaviour of a vertical well as well as a horizontal well located within an intersecting sealing fault and a constant pressure boundary. The methods employed in computing the dimensionless pressures and dimensionless pressure derivatives for both well types include the method of images and principle of superposition. Their results show that for the selected parameters; the models give accurate estimation of distances between active and image wells, for a given distance, both P_D and P_D' decrease as horizontal well length L increases. The longer the well length, the lower the drawdown required to give same effects, as would shorter lengths, on the well performance at a given time of production thereby prolonging production over time, the type curves can be used for matching of actual pressure drawdown data and determining the drainage area and relative well location with respect to physical boundaries.

Edobhiye O. and Adewole E.S. investigated the effects of both wellbore and reservoir properties on dimensionless pressure and dimensionless pressure derivatives of a horizontal well in a reservoir subject to bottom water, gas cap and single edge water drive mechanisms [7]. The effects of rectangular and square reservoir geometries were also considered in their study and the source and Green's functions together with the Newman's product rule were utilized. Results show that dimensionless pressure increases with reservoir thickness, dimensionless wellbore radius and dimensionless well length were found to be inversely related to dimensionless pressure. Ogbue M.C. considered all potential flow regimes of a horizontal well in a reservoir supported by bottom water drive [8]. The physical model and the mathematical model were developed based on the conceptual model. The pressure distribution is in the form of dimensionless pressure and dimensionless pressure derivative functions of reservoir system properties, fluid properties, reservoir system geometry and dimensionless time. Results of the study showed a series of flow patterns along the principal axes or along combinations of the principal axes. Each flow regime could be recognized by its characteristic signature in the log-log graph plots of the pressure distribution.

Ozkan Erdal and Raghavan Rajagopal discussed the performance of a horizontal well subject to bottom water drive and delineates conditions under which this completion mode is more appropriate [9]. They also discussed the productivities of horizontal wells operating under bottom water drive in terms of displacement efficiencies. This work presents information that enables the engineer to decide on the productivity improvements that may be expected from horizontal-well completions under bottom water drive. Their results showed the effect of a constant-pressure gas cap on well performances would be similar to that of an active aquifer at the bottom of the formation. Results and the discussions are also applicable to oil production by gas-cap drive. Ogbamikhumi A.V. and Adewole E.S. deployed analytical solution method of Green's and Source functions to determine the performance of a horizontal well located between two parallel sealing faults, assuming simple rectangular reservoir geometry [10]. The pressure expression derived from their work revealed that a maximum of two flow periods occur for the stated reservoir model. They discovered that increased perforation length reduces the production potential of the horizontal well.

Oloro J.O, Adewole E.S. analyzed a plot of dimensionless pressure versus dimensionless time on a log-log paper for six sets of data to illustrate the pressure distribution of horizontal wells in a two layered reservoir with simultaneous gas cap and bottom water drive [11]. From the graphs it was shown that dimensionless pressure increases with dimensionless time. They observed that when there is crossflow, pressure distribution in such reservoir is the same as that of the homogeneous system and pressure responses in crossflow reservoir are higher than that of without crossflow. Oloro J.O and Adewole S.E carried out a study using source functions and Newman's product rule to develop models to predict the performance and behavior of a horizontal well which was subjected by double Edgewater drive [12]. They used numerical methods to perform the computation and Sensitivity analysis of parameters. Their results showed that, the performance and behavior of the reservoir were found to be, when the well is positioned at well length (x_{wD}:y_{wD}: z_{wD}), in the ratio of 12:7:15 respectively.

Ogbue M.C. and Adewole E.S., their theoretical research aimed at solving for time water will breakthrough a horizontal well placed in bottom-water reservoir [13]. In their study, they suggested ways to delay the water breakthrough time. Thus, the model herein is a repository of three aims of reservoir modeling; predict, optimize and monitor oil production. Well modifications strategies were suggested to achieve significant delay of water breakthrough. Their results showed, from the mathematical model factors affecting water breakthrough were chiefly wellbore, reservoir fluid and reservoir properties. Water breakthrough was evidenced by constant P_D value. Delayed water breakthrough is favoured by narrow well, shorter well, low viscous fluid, low flow rate and high horizontal permeability relative to vertical permeability. Higher values of and t_{De} can be achieved by increasing the horizontal permeability, k_h while vertical permeability, k_v is reduced. Suitable stimulation process can achieve improved permeability. Oloro j. and Adewole E.S. determined the factors that affect pressure distribution of horizontal wells in a layered reservoir subjected to simultaneous gas-cap at the top and bottom water drives [14]. Well completion was carried out in a particular layer and one of the parameters was varied while the others were kept constant. The results show that the following factors; wellbore radius, well length and pay thickness affect pressure distribution in two-layered reservoir subject to both active gas cap and bottom water drive which affect pressure distribution. Further, results show slightly high productivity when smaller wellbore radius is used.

2. Reservoir Model Description

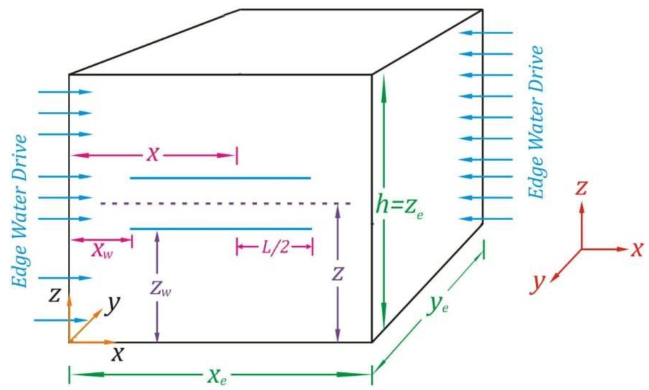

Figure 1. *Horizontal well in an anisotropic oil reservoir.*

3. Mathematical Model Description

At late time flow regime, the following are the corresponding source functions according to Alain C. Gringarten and Henry J. Ramey Jr (1973) in $x, y\ and\ z - axis$ respectively.

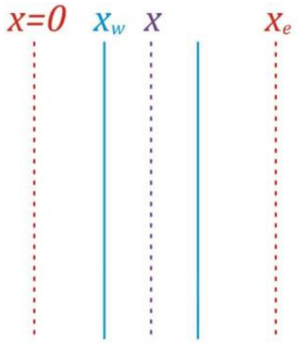

Figure 2. *Physical description of an anisotropic oil reservoir along the* $x - axis$.

$$s(x,t) = \frac{4}{\pi}\sum_{n=1}^{\infty}\frac{1}{n}exp\left(-\frac{n^2\pi^2\eta_x t}{x_e^2}\right)\sin\left(\frac{n\pi x_f}{2x_e}\right)\sin\left(\frac{n\pi x_w}{x_e}\right)\sin\left(\frac{n\pi x}{x_e}\right) \tag{1}$$

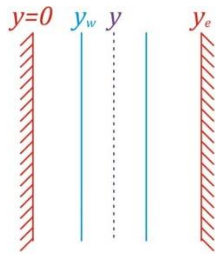

Figure 3. *Physical description of an anisotropic oil reservoir along the* $y{-}axis$.

$$s(y,t) = \frac{1}{y_e}\left[1 + 2\sum_{n=1}^{\infty}exp\left(-\frac{n^2\pi^2\eta_y t}{y_e^2}\right)\cos\left(\frac{n\pi y_w}{y_e}\right)\cos\left(\frac{n\pi y}{y_e}\right)\right] \tag{2}$$

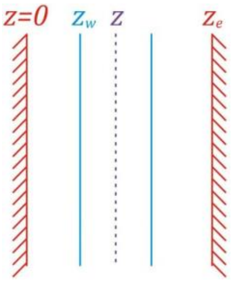

Figure 4. *Physical description of an anisotropic oil reservoir along the* $z - axis$.

$$s(z,t) = \frac{1}{z_e}\left[1 + 2\sum_{n=1}^{\infty}exp\left(-\frac{n^2\pi^2\eta_z t}{z_e^2}\right)\cos\left(\frac{n\pi z_w}{z_e}\right)\cos\left(\frac{n\pi z}{z_e}\right)\right] \tag{3}$$

Since $z_e = h$, we have;

$$s(z,t) = \frac{1}{h}\left[1 + 2\sum_{n=1}^{\infty}exp\left(-\frac{n^2\pi^2\eta_z t}{h^2}\right)\cos\left(\frac{n\pi z_w}{h}\right)\cos\left(\frac{n\pi z}{h}\right)\right] \tag{4}$$

Dimensionlizing the above equations we have: -

$$s(x_D,t_D)=\frac{4}{\pi}\sum_{n=1}^{\infty}\frac{1}{n}exp\left(-\frac{n^2\pi^2t_D}{x_{eD}^2}\right)\sin\left(\frac{n\pi}{x_{eD}}\sqrt{\frac{k}{k_x}}\right)\sin\left(\frac{n\pi x_{wD}}{x_{eD}}\right)\sin\left(\frac{n\pi x_D}{x_{eD}}\right) \tag{5}$$

$$s(y_D,t_D)=\frac{2}{y_{eD}}\sqrt{\frac{k}{k_y}}\left[1+2\sum_{n=1}^{\infty}exp\left(-\frac{n^2\pi^2t_D}{y_{eD}^2}\right)\cos\left(\frac{n\pi y_{wD}}{y_{eD}}\right)\cos\left(\frac{n\pi y_D}{y_{eD}}\right)\right] \tag{6}$$

$$s(z_D,t_D)=\frac{2}{h_D}\sqrt{\frac{k}{k_z}}\left[1+2\sum_{n=1}^{\infty}exp\left(-\frac{n^2\pi^2t_D}{h_D^2}\right)\cos\left(\frac{n\pi z_{wD}}{h_D}\right)\cos\left(\frac{n\pi z_D}{h_D}\right)\right] \tag{7}$$

Late linear flow regime
The late linear flow regime is governed by the equation;

$$P_D=2\pi h_D\int_0^{\tau_D}(Late\ x*Late\ y*Late\ z)d\tau \tag{8}$$

Using equations (5), (6) and (7) in equation (8) and simplifying we have:

$$P_D=\frac{4}{y_{eD}}\sqrt{\frac{k}{k_y}}\int_0^{\tau_D}\sum_{n=1}^{\infty}\frac{1}{n}exp\left(-\frac{n^2\pi^2t_{Di}}{x_{eD}^2}\right)\sin\left(\frac{n\pi}{x_{eD}}\sqrt{\frac{k}{k_x}}\right)\sin\left(\frac{n\pi x_{wD}}{x_{eD}}\right)\sin\left(\frac{n\pi x_D}{x_{eD}}\right)$$

$$*\left[1+2\sum_{n=1}^{\infty}exp\left(-\frac{n^2\pi^2t_{Di}}{y_{eD}^2}\right)\cos\left(\frac{n\pi y_{wD}}{y_{eD}}\right)\cos\left(\frac{n\pi y_D}{y_{eD}}\right)\right]*\left[1+2\sum_{n=1}^{\infty}exp\left(-\frac{n^2\pi^2t_{Di}}{h_D^2}\right)\cos\left(\frac{n\pi z_{wD}}{h_D}\right)\cos\left(\frac{n\pi z_D}{h_D}\right)\right]d\tau_D \tag{9}$$

The dimensionless pressure derivative at steady-state is given as [15]:

$$P_D'=t_D\frac{\partial P_D}{\partial t_D} \tag{10}$$

$$P_D'=\frac{4t_{Di}}{y_{eD}}\sqrt{\frac{k}{k_y}}\sum_{n=1}^{\infty}\frac{1}{n}exp\left(-\frac{n^2\pi^2t_{Di}}{x_{eD}^2}\right)\sin\left(\frac{n\pi}{x_{eD}}\sqrt{\frac{k}{k_x}}\right)\sin\left(\frac{n\pi x_{wD}}{x_{eD}}\right)\sin\left(\frac{n\pi x_D}{x_{eD}}\right)$$

$$*\left[1+2\sum_{n=1}^{\infty}exp\left(-\frac{n^2\pi^2t_{Di}}{y_{eD}^2}\right)\cos\left(\frac{n\pi y_{wD}}{y_{eD}}\right)\cos\left(\frac{n\pi y_D}{y_{eD}}\right)\right]*\left[1+2\sum_{n=1}^{\infty}exp\left(-\frac{n^2\pi^2t_{Di}}{h_D^2}\right)\cos\left(\frac{n\pi z_{wD}}{h_D}\right)\cos\left(\frac{n\pi z_D}{h_D}\right)\right] \tag{11}$$

Integrating the equations for the late linear flow regime, the P_D and P_D' equations are outlined below:
Considering the following as shown in table 1;

$$r_{wD}=z_D-z_{wD},\ z_{eD}=2z_{wD}=h_D,\ x_D=x_{wD},\ y_D=y_{wD}\ \text{and}\ 2y_D=2y_{wD}=y_{eD}; \tag{12}$$

Integrating the above equations we have;

$$P_D=\frac{\alpha_2}{y_{eD}}\left(1-e^{-\alpha_1t_{Di}}\right) \tag{13}$$

$$P_D'=\frac{\alpha_3t_{Di}}{y_{eD}}e^{-\alpha_1t_{Di}} \tag{14}$$

Where;

$$\alpha_1=\frac{\pi^2}{x_{eD}^2}\sin\left(\frac{\pi}{x_{eD}}\sqrt{\frac{k}{k_x}}\right)\sin\left(\frac{\pi x_{wD}}{x_{eD}}\right)\sin\left(\frac{\pi x_D}{x_{eD}}\right);\ \alpha_2=\frac{36}{\alpha_1}\sqrt{\frac{k}{k_y}};\ \alpha_3=36\sqrt{\frac{k}{k_y}} \tag{15}$$

When calculating x_{eD}, for corresponding L_i,

$$x_{e_i}=x_e-2x_i\ \text{where}\ 1\le i\le 8 \tag{16}$$

For large t_{Di};

$$P_D=\frac{\alpha_2}{y_{eD}};\ P_D'=0 \tag{17}$$

4. Methodology and Demonstration of the Problem

In this study, for the interpretation of the results we have used the cubic spline data interpolation. Splines are popular curves which are simple to construct and are characterized by accuracy of evaluation, ease and capacity to approximate complex shapes, interactive curve design and curve fitting. Consider the following numerical data of reservoir, wellbore and fluid properties in an anisotropic oil reservoir: -

$$L = 1000ft, 2000ft, 3000ft, 4000ft, 5000ft, 6000ft, 7000ft, 8000ft$$

$x = x_w = 224.7ft, d_x = 224.7ft,\ D_x = 1224.7ft,\ y = y_w = 7000ft, d_y = 7000ft,\ D_y = 7001ft,\ z = 275.5ft,\ z_w = 275ft,$

$d_z = 275ft,\ D_z = 276ft,\ x_e = 9000ft, y_e = 14000ft,\ z_e = h = 550ft$, $k_x = 156md, k_y = 210md, k_z = 220md$, $\sqrt{\frac{k}{k_x}} = 1.1127,\ \sqrt{\frac{k}{k_y}} = 0.9591,\ \sqrt{\frac{k}{k_z}} = 0.9370,\ \sqrt{\frac{k_h}{k_v}} = 0.9070,\ k = \sqrt[3]{k_x.k_y.k_z} = 193.16md$, For a horizontal well; $k_v > k_h$ where $k_v = k_z$ and $k_h = \sqrt{k_x k_y} = 181md$

Table 1. *Calculated dimensionless reservoir, wellbore and fluid properties,* $x_D = 0.5000$.

Dimensionless parameter	$L(ft)$	1000	2000	3000	4000	5000	6000	7000	8000
	L_D	1.0115	2.0231	3.0346	4.0462	5.0577	6.0693	7.0808	8.0924
	h_D	1.03070	0.51535	0.34357	0.25768	0.20614	0.17178	0.14724	0.12884
x_D		0.5000	0.5000	0.5000	0.5000	0.5000	0.5000	0.5000	0.5000
y_D		13.4274	6.7137	4.4758	3.35685	2.68553	2.2379	1.9182	1.678425
z_D		0.516287	0.258144	0.172096	0.129072	0.103257	0.086048	0.073755	0.064536
x_{wD}		0.5000	0.5000	0.5000	0.5000	0.5000	0.5000	0.5000	0.5000
y_{wD}		13.4274	6.7137	4.4758	3.35685	2.68553	2.2379	1.9182	1.678425
z_{wD}		0.515350	0.257675	0.171785	0.128840	0.103070	0.085890	0.073620	0.064420
x_{eD}		19.0285	9.0142	5.6761	4.0071	3.0056	2.3380	1.8611	1.5035
y_{eD}		26.8548	13.4274	8.9516	6.7137	5.37106	4.4758	3.8364	3.35685
z_{eD}		1.03070	0.51535	0.34357	0.25768	0.20614	0.17178	0.14724	0.12884
r_{wD}		0.000937	0.000469	0.000311	0.000232	0.000187	0.000158	0.000135	0.000116
α_1		0.0000339	0.00138	0.0132	0.0687	0.2499	0.6975	1.5167	2.3798
$\propto_2$		1018513.274	25020	2615.727273	502.5851528	138.1656663	49.50193548	22.76495022	14.50861417
$\propto_3$		34.5276	34.5276	34.5276	34.5276	34.5276	34.5276	34.5276	34.5276

Table 2. P_D *and* P'_D *with varying dimensionless time,* t_D *and dimensionless well length,* L_D *respectively.*

	L_D	1.0115	2.0231	3.0346	4.0462
	y_{eD}	26.8548	13.4274	8.9516	6.7137
	h_D	1.03070	0.51535	0.34357	0.25768
t_D	x_D	0.5000	0.5000	0.5000	0.5000
	α_1	0.0000339	0.00138	0.0132	0.0687
	α_2	1018513.274	25020	2615.727273	502.5851528
	$\propto_3$	34.5276	34.5276	34.5276	34.5276

	P_D	P'_D	P_D	P'_D	P_D	P'_D	P_D	P'_D
0.0000	0.0000	0.0000	0.0000	0.0000	0.0000	0.0000	0.0000	0.0000
1.00E+00	1.2857	1.2857	2.5697	2.5679	3.8318	3.8066	4.9702	4.8014
1.00E+01	12.8550	12.8528	25.5377	25.3619	36.1341	33.8017	37.1990	25.8728
1.00E+02	128.3537	128.1363	240.1888	223.9968	214.1488	103.0379	74.7819	0.5341
1.00E+03	1264.1656	1242.8591	1394.5741	646.9163	292.2073	7.14E-03	74.8596	7.50E-27
1.00E+04	10904.5847	9160.4886	1863.3521	0.0261	292.2078	1.82E-53	74.8596	0
1.00E+05	36648.2171	4333.9727	1863.3540	3.00E-55	292.2078	0	74.8596	0
1.00E+06	37926.6751	2.44E-09	1863.3540	0	292.2078	0	74.8596	0
1.00E+07	37926.6751	0	1863.3540	0	292.2078	0	74.8596	0
1.00E+08	37926.6751	0	1863.3540	0	292.2078	0	74.8596	0
1.00E+09	37926.6751	0	1863.3540	0	292.2078	0	74.8596	0
1.00E+10	37926.6751	0	1863.3540	0	292.2078	0	74.8596	0
	L_D	5.0577	6.0693		7.0808		8.0924	
	y_{eD}	5.37106	4.4758		3.8364		3.35685	
	h_D	0.20614	0.17178		0.14724		0.12884	
t_D	x_D	0.5000	0.5000		0.5000		0.5000	
	α_1	0.2499	0.6975		1.5167		2.3798	
	α_2	138.1656663	49.50193548		22.76495022		14.50861417	
	$\propto_3$	34.5276	34.5276		34.5276		34.5276	
	P_D	P'_D	P_D	P'_D	P_D	P'_D	P_D	P'_D
0.0000	0.0000	0.0000	0.0000	0.0000	0.0000	0.0000	0.0000	0.0000
1.00E+00	5.6881	5.0070	5.5540	3.8404	4.6318	1.9749	3.9220	0.9521
1.00E+01	23.6104	5.2821	11.0496	0.0721	5.9339	2.33E-05	4.3221	4.75E-09
1.00E+02	25.7241	9.02E-09	11.0599	3.94E-28	5.9339	1.22E-63	4.3221	0
1.00E+03	25.7241	0	11.0599	0	5.9339	0	4.3221	0
1.00E+04	25.7241	0	11.0599	0	5.9339	0	4.3221	0
1.00E+05	25.7241	0	11.0599	0	5.9339	0	4.3221	0
1.00E+06	25.7241	0	11.0599	0	5.9339	0	4.3221	0
1.00E+07	25.7241	0	11.0599	0	5.9339	0	4.3221	0
1.00E+08	25.7241	0	11.0599	0	5.9339	0	4.3221	0
1.00E+09	25.7241	0	11.0599	0	5.9339	0	4.3221	0
1.00E+10	25.7241	0	11.0599	0	5.9339	0	4.3221	0

Table 3. *P_D and P'_D with varying dimensionless time, t_D; $L_D = 1.0115$.*

	L_D	1.0115
	y_{eD}	26.8548
t_D	h_D	1.03070
	x_Dl	0.5000

	α_1	0.0000339
	α_2	1018513.274
	$\propto_3$	34.5276
	P_D	P_D'
0	0	0
50000	30963.3668	11802.8076
100000	36648.2171	4333.9727
150000	37691.9512	1193.5711
200000	37883.5800	292.1850
250000	37918.7629	67.0562
300000	37925.2224	14.7738
350000	37926.4084	3.1645
400000	37926.6261	0.6640
450000	37926.6661	0.1371
500000	37926.6734	0.0280
550000	37926.6748	0.0057
600000	37926.6750	0.0011
650000	37926.6751	0.0002
700000	37926.6751	0.0000

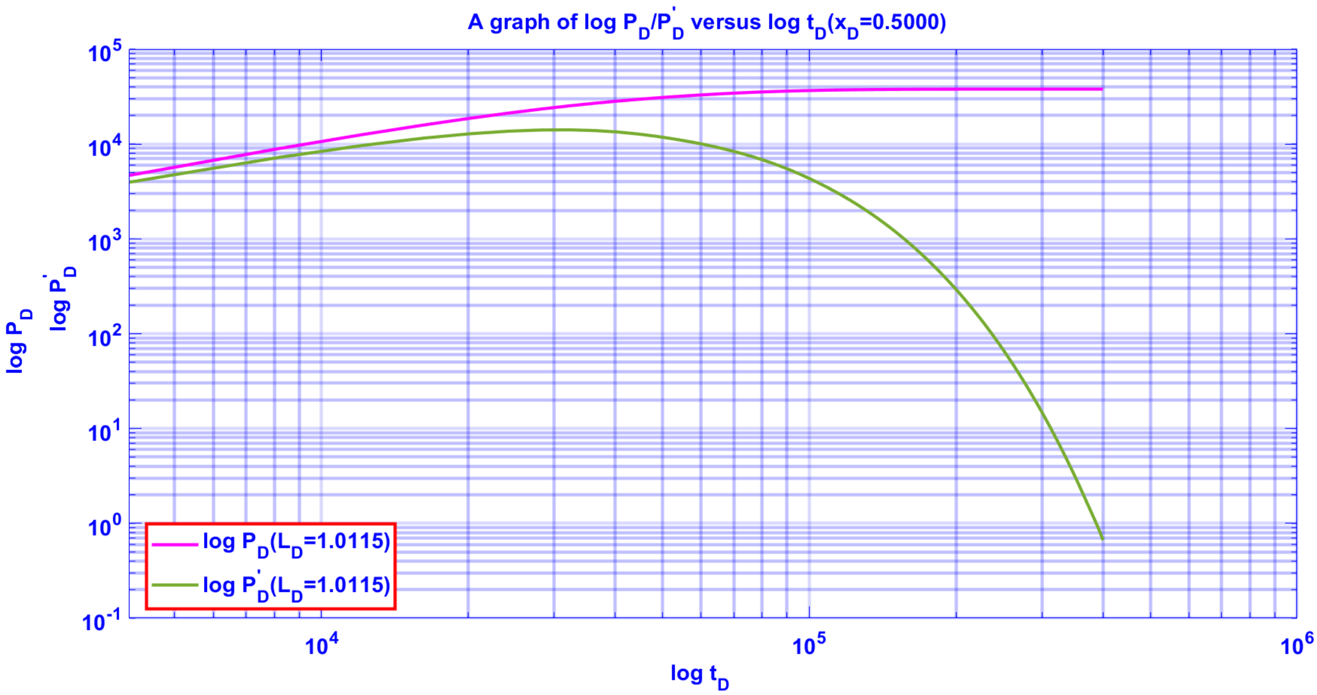

Figure 5. *Graph of log* P_D *and log* P'_D *with varying log* t_D *for* $L_D = 1.0115$.

Table 4. P_D and P'_D with varying dimensionless time, t_D; $L_D = 2.0231$.

t_D	L_D	2.0231
	y_{eD}	13.4274
	h_D	0.51535
	x_D	0.5000
	α_1	0.00138
	α_2	25020
	$\propto_3$	34.5276
	P_D	P'_D
0	0	0
1500	1628.2253	486.7166
3000	1833.6841	122.8334
4500	1859.6101	23.2497
6000	1862.8816	3.9117
7500	1863.2944	0.6170
9000	1863.3465	0.0934
10500	1863.3531	0.0138
12000	1863.3539	0.0020
13500	1863.3540	0.0003
15000	1863.3540	0.0000

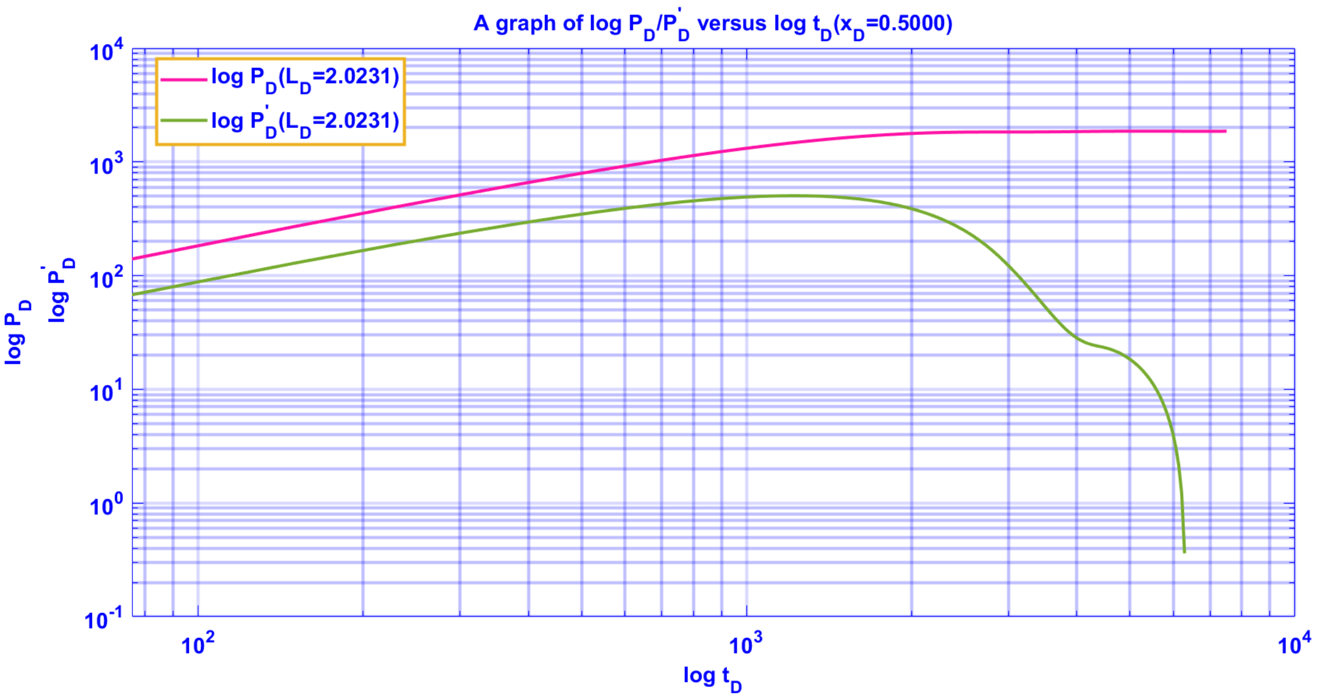

Figure 6. Graph of log P_D and log P'_D with varying log t_D for $L_D = 2.0231$.

Table 5. *P_D and P'_D with varying dimensionless time, t_D; $L_D = 3.0346$.*

	L_D	3.0346
	y_{eD}	8.9516l
	h_D	0.34357
t_D	x_D	0.5000
	α_1	0.0132
	α_2	2615.727273
	$\propto_3$	34.5276
	P_D	P_D'
0	0	0
100	214.1488	103.0379
200	271.3555	55.0501
300	286.6374	22.0587
400	290.7197	7.8569
500	291.8103	2.6236
600	292.1016	0.8410
700	292.1794	0.2621
800	292.2002	0.0800
900	292.2058	0.0240
1000	292.2073	0.0071
1100	292.2076	0.0021
1200	292.2078	0.0006
1300	292.2078	0.0002
1400	292.2078	0.0001
1500	292.2078	0.0000

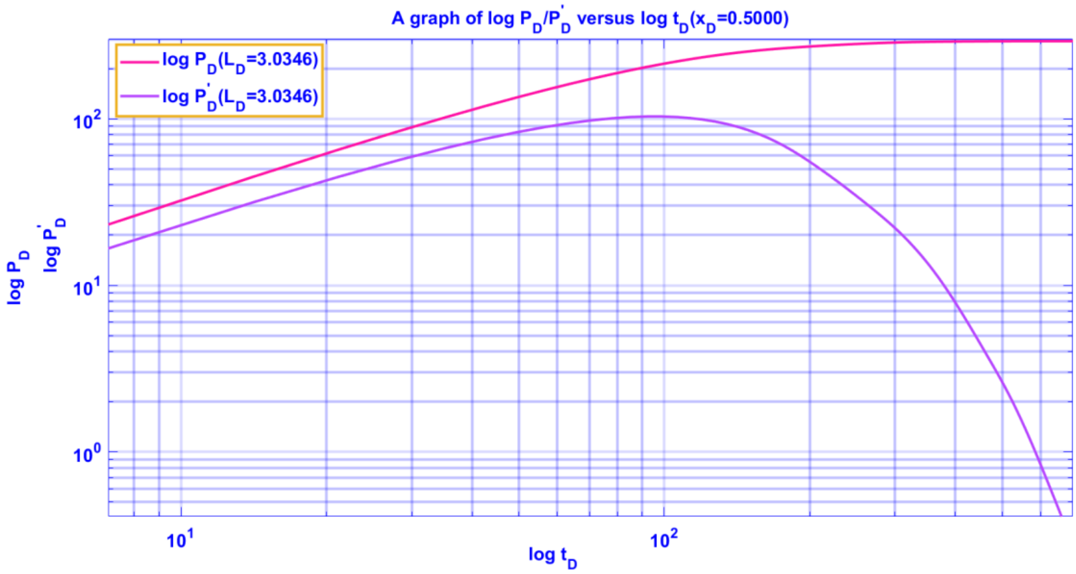

Figure 7. *Graph of log P_D and log P'_D with varying log t_D for $L_D = 3.0346$.*

Table 6. *P_D and P'_D with varying dimensionless time, t_D; $L_D = 4.0462$.*

	L_D	4.0462
	y_{eD}	6.7137
	h_D	0.25768
t_D	x_D	0.5000
	α_1	0.0687
	α_2	502.5851528
	$\propto_3$	34.5276
	P_D	P'_D
0	0	0
25	61.4213	23.0804
50	72.4473	8.2865
75	74.4266	2.2313
100	74.7819	0.5341
125	74.8457	0.1198
150	74.8571	0.0258
175	74.8592	0.0054
200	74.8596	0.0011
225	74.8596	0.0002
250	74.8596	0.0000
275	74.8596	0.0000
300	74.8596	0.0000

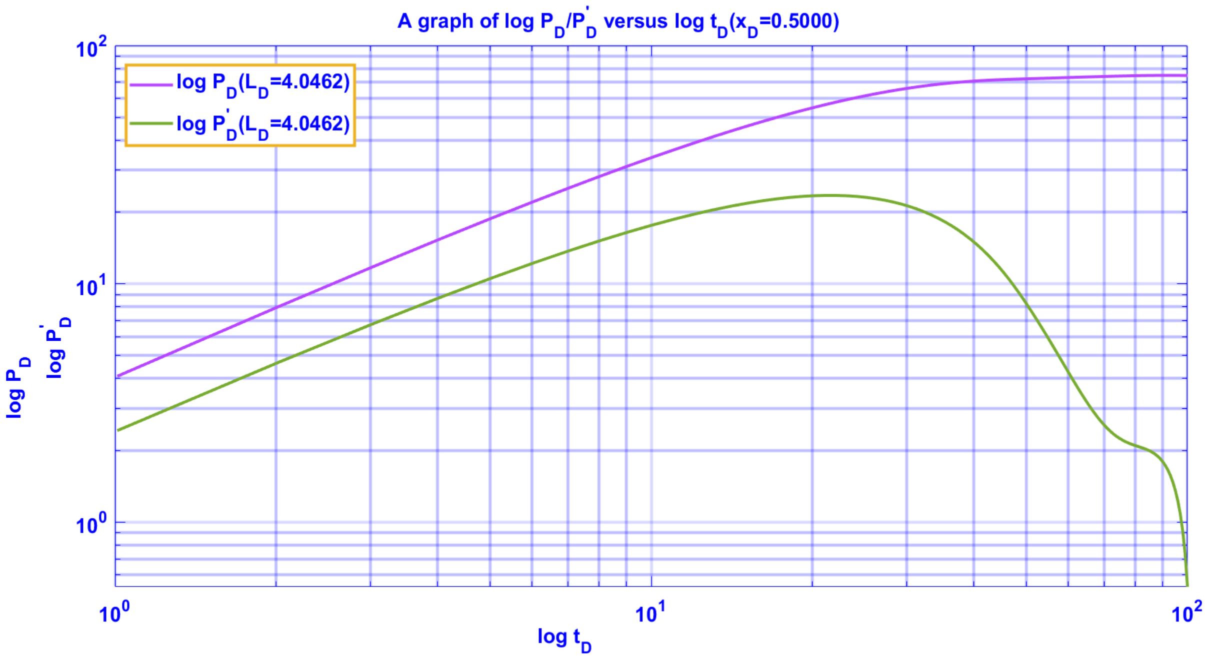

Figure 8. *Graph of log P_D and log P'_D with varying log t_D for $L_D = 4.0462$.*

Table 7. *P_D and P'_D with varying dimensionless time, t_D; $L_D = 5.0577$.*

	L_D	5.0577
	y_{eD}	5.37106
	h_D	0.20614
t_D	x_D	0.5000
	α_1	0.2499
	α_2	138.1656663
	$\propto_3$	34.5276
	P_D	P_D'
0.0	0	0
2.5	11.9515	8.6044
5.0	18.3503	9.2135
7.5	21.7762	7.3993
10.0	23.6104	5.2821
12.5	24.5924	3.5350
15.0	25.1182	2.2711
17.5	25.3997	1.4186
20.0	25.5504	0.8680
22.5	25.6311	0.5228
25.0	25.6743	0.3110
27.5	25.6974	0.1832
30.0	25.7098	0.1070
32.5	25.7165	0.0621
35.0	25.7200	0.0358
37.5	25.7219	0.0205
40.0	25.7229	0.0117

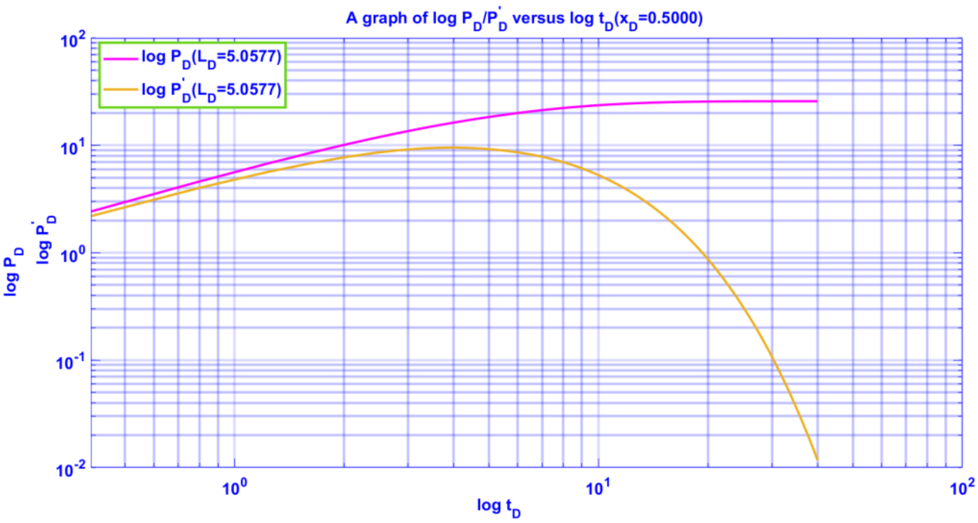

Figure 9. *Graph of log P_D and log P'_D with varying log t_D for $L_D = 5.0577$.*

Table 8. *P_D and P'_D with varying dimensionless time, t_D; $L_D = 6.0693$.*

t_D	L_D	6.0693
	y_{eD}	4.4758
	h_D	0.17178
	x_D	0.5000
	α_1	0.6975
	α_2	49.50193548
	$\propto_3$	34.5276
	P_D	P'_D
0	0	0
2	8.3189	3.8237
4	10.3806	1.8953
6	10.8916	0.7046
8	11.0182	0.2328
10	11.0496	0.0721
12	11.0573	0.0215
14	11.0593	0.0062
16	11.0598	0.0018
18	11.0599	0.0005
20	11.0599	0.0001
22	11.0599	0.0000

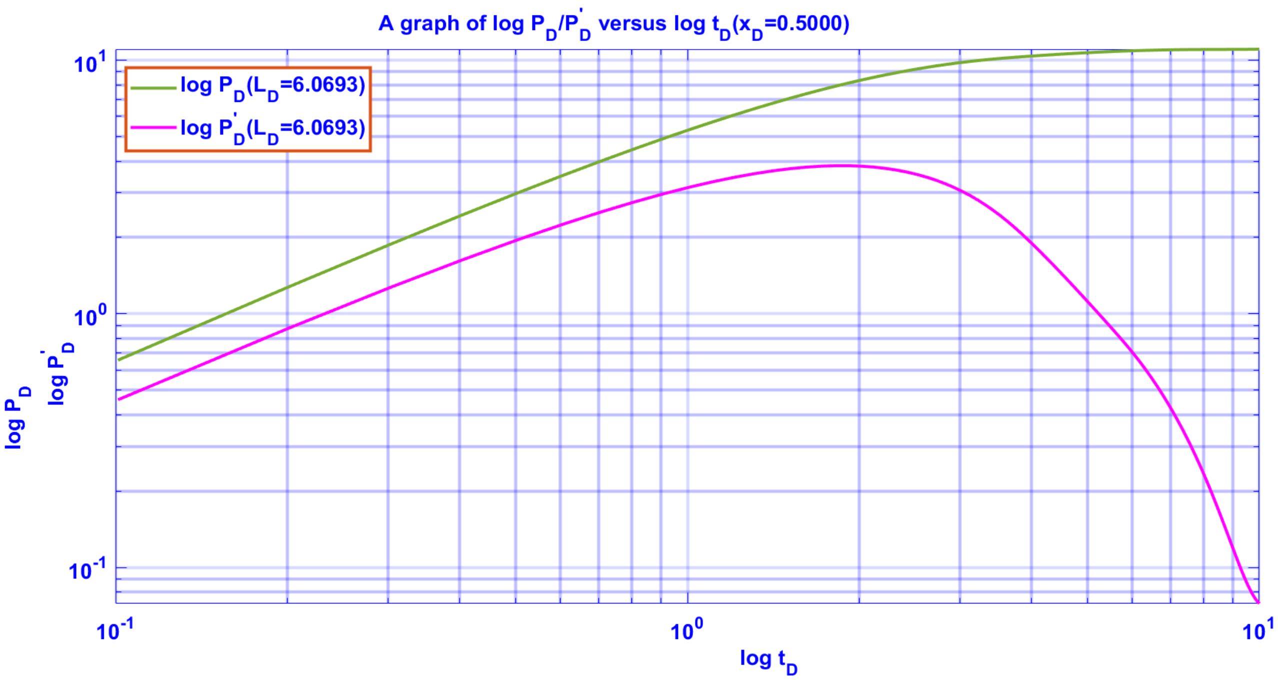

Figure 10. *Graph of log P_D and log P'_D with varying log t_D for $L_D = 6.0693$.*

Table 9. *P_D and P'_D with varying dimensionless time, t_D; $L_D = 7.0808$.*

t_D	L_D	7.0808
	y_{eD}	3.8364
	h_D	0.14724
	x_D	0.5000
	α_1	1.5167
	α_2	22.76495022
	$\propto_3$	34.5276
	P_D	P'_D
0	0	0
1	4.6318	1.9749
2	5.6482	0.8667
3	5.8712	0.2853
4	5.9202	0.0835
5	5.9309	0.0229
6	5.9333	0.0060
7	5.9338	0.0015
8	5.9339	0.0004
9	5.9339	0.0001
10	5.9339	0.0000

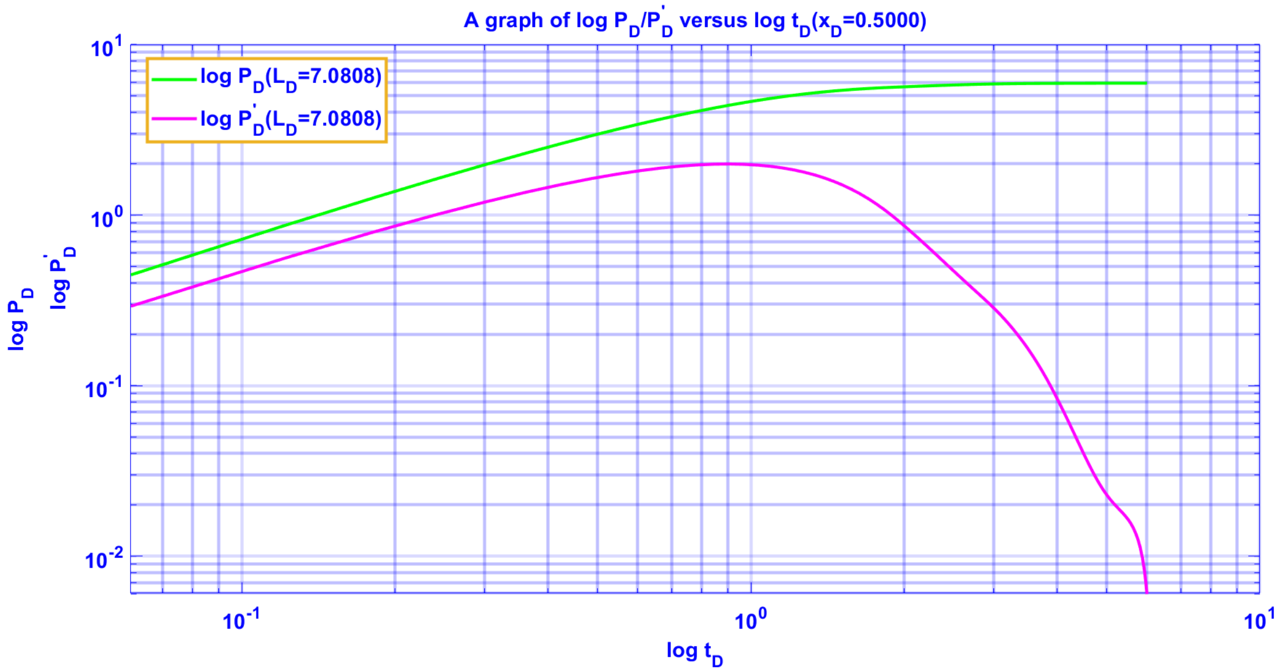

Figure 11. *Graph of log P_D and log P'_D with varying log t_D for $L_D = 7.0808$.*

Table 10. *P_D and P'_D with varying dimensionless time, t_D; $L_D = 8.0924$.*

t_D	L_D	8.0924
	y_{eD}	3.35685
	h_D	0.12884
	x_D	0.5000
	α_1	2.3798
	α_2	14.50861417
	$\propto_3$	34.5276
	P_D	P'_D
0.0	0.0000	0.0000
0.5	3.0071	1.5647
1.0	3.9220	0.9521
1.5	4.2004	0.4345
2.0	4.2851	0.1763
2.5	4.3108	0.0670
3.0	4.3187	0.0245
3.5	4.3210	0.0087
4.0	4.3218	0.0030
4.5	4.3220	0.0010
5.0	4.3221	0.0003
5.5	4.3221	0.0001
6.0	4.3221	0.0000

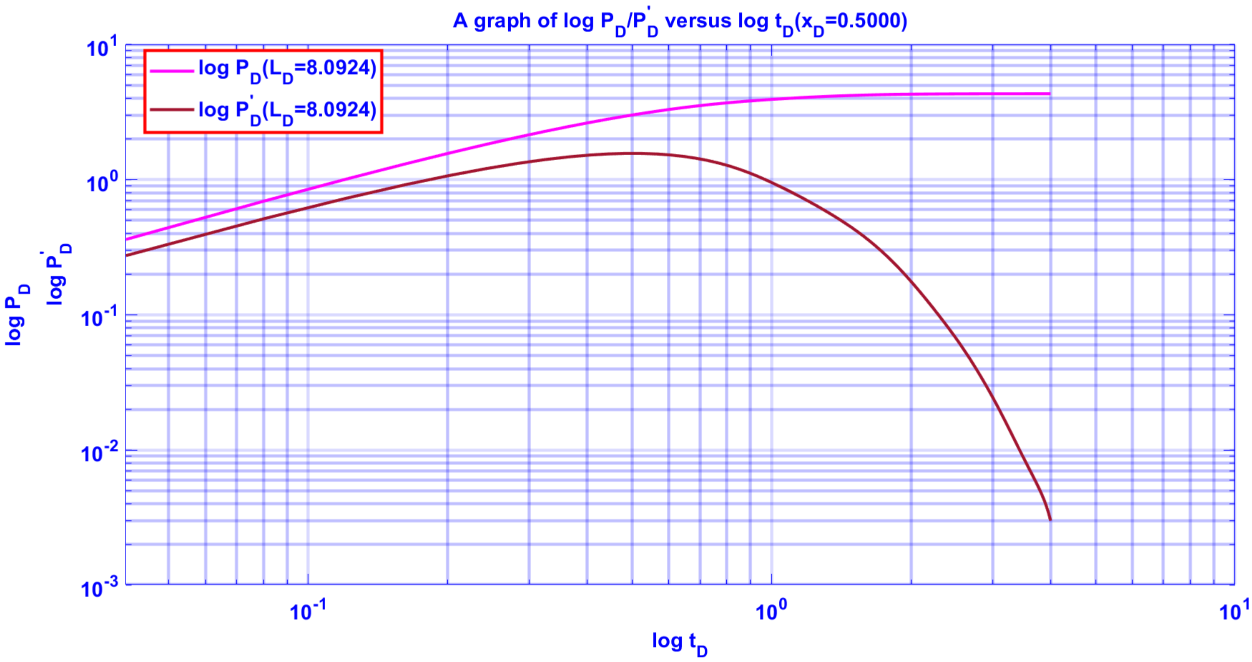

Figure 12. *Graph of log P_D and log P'_D with varying log t_D for $L_D = 8.0924$.*

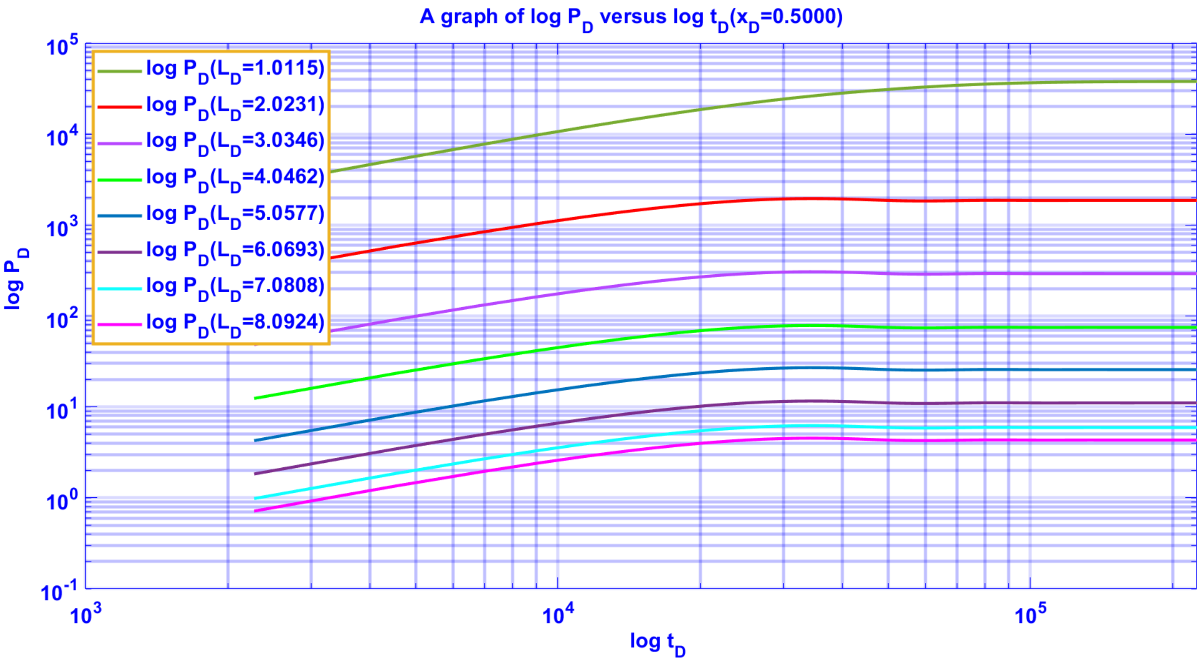

Figure 13. *Graph of log P_D with varying log t_D for all dimensionless well length, L_D.*

Table 11. *P_D and P'_D with varying dimensionless time, t_D; $L_D = 6.0693$, $L_D = 7.0808$, $L_D = 8.0924$.*

	L_D	6.0693		7.0808		8.0924	
	y_{eD}	4.4758		3.8364		3.35685	
	h_D	0.17178		0.14724		0.12884	
t_D	x_D	0.5000		0.5000		0.5000	
	α_1	0.6975		1.5167		2.3798	
	α_2	49.50193548		22.76495022		14.50861417	
	$\propto_3$	34.5276		34.5276		34.5276	
	P_D	P'_D	P_D	P'_D	P_D	P'_D
0.0	0.0000	0.0000	0.0000	0.0000	0.0000	0.0000
0.5	3.2564	2.7215	3.1543	2.1080	3.0071	1.5647
1.0	5.5540	3.8404	4.6318	1.9749	3.9220	0.9521
1.5	7.1751	4.0645	5.3240	1.3877	4.2004	0.4345
2.0	8.3189	3.8237	5.6482	0.8667	4.2851	0.1763
2.5	9.1259	3.3724	5.8001	0.5075	4.3108	0.0670
3.0	9.6954	2.8553	5.8712	0.2853	4.3187	0.0245
3.5	10.0971	2.3504	5.9046	0.1559	4.3210	0.0087
4.0	10.3806	1.8953	5.9202	0.0835	4.3218	0.0030
4.5	10.5806	1.5044	5.9275	0.0440	4.3220	0.0010
5.0	10.7217	1.1794	5.9309	0.0229	4.3221	0.0003
5.5	10.8213	0.9154	5.9325	0.0118	4.3221	0.0001
6.0	10.8916	0.7046	5.9333	0.0060	4.3221	0.0000

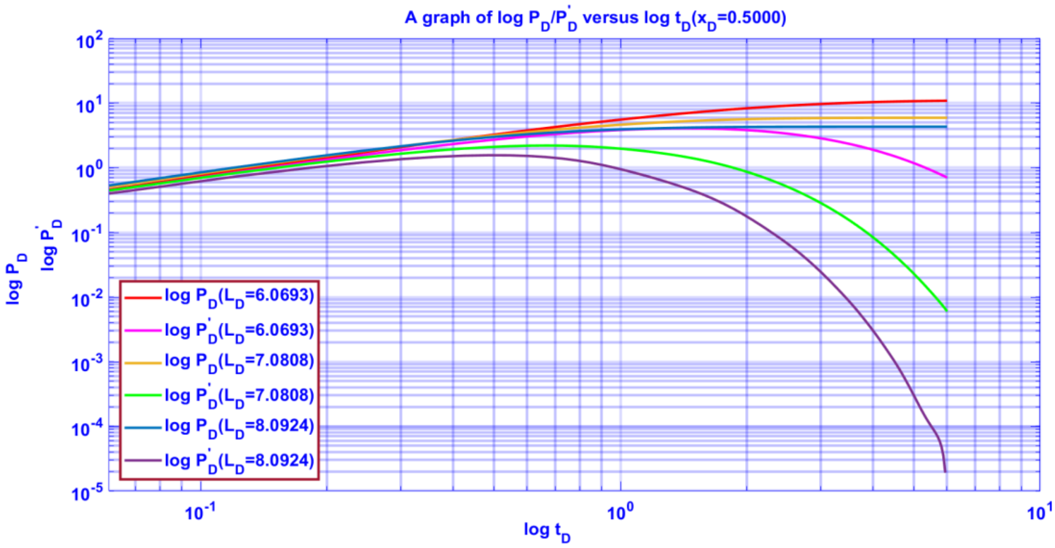

Figure 14. *Graph of log* P_D/P'_D *with varying log* t_D *for various dimensionless well length,* L_D*.*

Table 12. P_{DBr} *and* t_{DBr} *with varying dimensionless well length,* L_D*, Dimensionless pay thickness,* h_D *and Dimensionless well width,* y_{eD}*.*

Dimensionless well length, L_D	1.0115	2.0231	3.0346	4.0462	5.0577	6.0693	7.0808	8.0924
Dimensionless pay thickness, h_D	1.03070	0.51535	0.34357	0.25768	0.20614	0.17178	0.14724	0.12884
Dimensionless well width, y_{eD}	26.8548	13.4274	8.9516	6.7137	5.37106	4.4758	3.8364	3.35685
Dimensionless fluid breakthrough time, t_{DBr}	700000	15000	1500	260	70	20.5	9.5	6
Dimensionless pressure at fluid breakthrough time, P_{DBr}	37926.7	1863.4	292.2	74.9	25.7	11.1	5.9	4.3

5. Results and Discussions

Table 1 defines the dimensionless parameters calculated at $x_D = 0.5000$. The results show that $x_D = x_{wD}$, $y_D = y_{wD}$, $2y_D = 2y_{wD} = y_{eD}$, $z_{eD} = 2z_{wD} = h_D$ and $r_{wD} = z_D - z_{wD}$.

Table 2 shows how dimensionless pressure, P_D and dimensionless pressure derivative, P'_D varies with dimensionless time, t_D for various dimensionless well length, L_D. Results show that dimensionless pressure, P_D is maximum when the dimensionless well length, L_D is minimum and vice versa. The dimensionless pressure derivative, P'_D collapses to zero when the dimensionless pressure, P_D starts to exhibit a constant trend signifying the encroachment of the unwanted fluid breakthrough.

Tables 3-5 describe precisely the relation between dimensionless pressure, P_D and dimensionless pressure derivative, P'_D with dimensionless time, t_D for $1.0115 < L_D < 8.0924$ with the idea of identifying the external fluid breakthrough time, t_{DBr}. Results show that the dimensionless pressure, P_{DBr} varies as fluid breakthrough time, t_{DBr} that is, $t_{DBr} \propto P_{DBr}$.

Table 6 show how dimensionless pressure, P_D and dimensionless pressure derivative, P'_D varies for various dimensionless well length, L_D with varying dimensionless time, t_D. Results indicate that, when dimensionless well length, L_D increase, dimensionless pressure, P_D decreases. Further all the results show that, when dimensionless pressure, P_D attains a constant trend, dimensionless pressure derivative, P'_D reduces to zero.

Table 7 summarizes Dimensionless fluid breakthrough time, t_{DBr} and Dimensionless pressure at fluid breakthrough time, P_{DBr} in relation to varying Dimensionless well length, L_D, Dimensionless pay thickness, h_D and Dimensionless well width, y_{eD}. Results show that, $t_{DBr} \propto P_{DBr}$ and $P_{DBr} \propto \frac{h_D y_{eD}}{L_D}$.

Figure 1 shows a horizontal well in an anisotropic oil reservoir. The well is eccentric to the reservoir to avoid early encroachment of the unwanted fluid (water). The well design enhances the clean oil production resulting to optimized production and enhanced oil recovery.

Figure 2 shows $x - axis$ physical description of a reservoir bounded at the bottom and at the top by simultaneous double edge sealing faults with constant pressure boundaries.

Figure 3 and figure 4 shows $y - axis$ and $z - axis$ physical description of a reservoir sealed at both ends simultaneously.

Figure 5 to figure 12 shows $log - log$ plots of P_D and P'_D with varying t_D. Further, the figures illustrate that, when the P_D starts to exhibit a constant trend, the P'_D collapses to zero implying fluid breakthrough time have been realized.

Figure 13 shows $log - log$ plot of P_D versus t_D for varying dimensionless well length, L_D. From the results, the dimensionless pressure, P_D increases with corresponding decrease in dimensionless well length, L_D. The dimensionless pressure, P_D is maximum when the dimensionless well length, L_D is minimum.

Figure 14 shows $log - log$ plots of P_D and P'_D with varying t_D for various dimensionless well length, L_D. The result show that when the dimensionless pressure, P_D starts to exhibit a constant trend, the dimensionless pressure derivative, P'_D collapses to zero indicating the encroachment of the unwanted external fluid (water).

6. Conclusions

1) Dimensionless fluid breakthrough time, t_{DBr} and dimensionless pressure at fluid breakthrough time, P_{DBr} varies as h_D and y_{eD} and inversely as L_D i.e $t_{DBr} \propto \frac{h_D y_{eD}}{L_D}$; $t_{DBr} \propto P_{DBr}$.
2) Minimum dimensionless well length, L_D provided the maximum dimensionless wellbore pressure, P_D.
3) Maximum dimensionless pay thickness, h_D provided the largest dimensionless wellbore pressure, P_D.
4) Largest dimensionless well width, y_{eD} produced the highest dimensionless wellbore pressure, P_D.
5) Dimensionless pressure, P_{DBr} at fluid breakthrough time, t_{DBr} is maximum for small dimensionless well length, L_D.
6) Calculated dimensionless reservoir, wellbore and fluid properties at $x_D = 0.5000$ shows; $r_{wD} = z_D - z_{wD}$, $z_{eD} = 2z_{wD} = h_D$, $y_D = y_{wD}$, $x_D = x_{wD}$ and $2y_D = 2y_{wD} = y_{eD}$.
7) Dimensionless pressure varies directly as x_{eD}^2 and inversely as y_{eD}, $P_D \propto x_{eD}^2 / y_{eD}$.

7. Recommendations

1) Reservoir engineers and petroleum engineers should drill the horizontal well with $1.0115 \leq L_D \leq 2.0231$, that is $1000\,ft \leq L \leq 2000\,ft$.
2) Prolonged dimensionless well length, L_D reduces the fluid breakthrough time which mar clean oil production.
3) Well eccentricity, where the horizontal well is located away from the double edge water drive boundaries offer delayed external fluid breakthrough time for the well completions.

Abbreviations

AJER	American Journal of Engineering Research
AMR	Advanced Materials Research
JPGE	Journal of Petroleum and Gas Engineering
NIJOTECH	Nigerian Journal of Technology
SPE	Society of Petroleum Engineers
SPEJ	Society of Petroleum Engineering Journal
USA	United States of America

Author Contributions

Mutili Peter Mutisya is the sole author. The author read and approved the final manuscript.

Conflicts of Interest

The author declares no conflicts of interest.

Appendix

Appendix I: Nomenclature

x *reservoir distance in the* $x - axis, ft$

x_D *dimensionless reservoir lateral distance on the* $x - axis$

y *reservoir distance in the* $y - axis, ft$

y_D *dimensionless reservoir lateral distance on the* $y - axis$

z *reservoir distance in the* $z - axis, ft$

z_D *dimensionless reservoir lateral distance on the* $z - axis$

x_e *half the distance to the boundary in the* $x - direction$

y_e *half the distance to the boundary in the* $y - direction$

x_w *the X coordinate of the production point*

y_w *the Y coordinate of the production point*

z_w *the Z coordinate of the production point*

z_D *the dimensionless distance from the bottom of the reservoir to the centre of the wellbore*

z_{wD} *the dimensionless distance from the bottom of the reservoir to the bottom of the wellbore*

x_{eD} *dimensionless external reservoir lateral extent on* $x - axis$

y_{eD} *dimensionless external reservoir lateral extent on* $y - axis$

z_{eD} *dimensionless external reservoir lateral extent on* $z - axis$

t_{DBr} *dimensionless fluid breakthrough time*

P_{DBr} *dimensionless pressure at fluid breakthrough time*

d_x the shortest distance between the well and the $x-$boundary, ft

d_y the shortest distance between the well and the $y-$boundary, ft

d_z the shortest distance between the well and the $z-$boundary, ft

D_x the longest distance between the well and the $x-$boundary, ft

D_y the longest distance between the well and the $y-$boundary, ft

D_z the longest distance between the well and the $z-$boundary, ft

r_w wellbore radius, ft

r_{wD} dimensionless wellbore radius

B oil formation volume factor, rbbl/STB

c_t total compressibility, 1/psi

i axial flow directions x, y, or z

h reservoir pay thickness, ft

h_D dimensionless reservoir height

k average reservoir permeability, md

k_i formation permeability in the i^{th} direction, md

k_h reservoir permeability in the horizontal axis, md

k_v reservoir permeability in the vertical axis, md

L total length of horizontal well, ft.

L_D dimensionless well length

P pressure, psi

ΔP pressure drop, psi

P_D dimensionless pressure at any point in the reservoir

P_D' dimensionless pressure derivative at any point in the reservoir

q flow rate, bbl/day

s source

t flow time, hours

t_D dimensionless time

D dimensionless

e external

w wellbore

Δ change

Appendix II: Greek Symbols

μ reservoir fluid viscosity, cp

τ dummy variable of time

τ_D dummy dimensionless time integration variable

η diffusivity constant, md-psi/cp

ϕ porosity, fraction

Appendix III: Dimensionless Parameters

$$P_D = \frac{kh\Delta p}{141.2q\mu B}$$

$$t_D = \frac{4kt}{\phi\mu c_t L^2}$$

$$\eta_i = \frac{k_i}{\phi\mu c_t}$$

$$i_D = \frac{2i}{L}\sqrt{\frac{k}{k_i}}$$

$$i_{wD} = \frac{2i_w}{L}\sqrt{\frac{k}{k_i}}$$

$$i_{eD} = \frac{2i_e}{L}\sqrt{\frac{k}{k_i}}$$

$$i = x, y, z$$

$$h_D = \frac{2h}{L}\sqrt{\frac{k}{k_z}}$$

$$L_D = \frac{L}{2h}\sqrt{\frac{k}{k_x}}$$

$$h_D = \frac{1}{L_D}\sqrt{\frac{k^2}{k_x k_z}}$$

$$r_{wD} = z_D - z_{wD}$$

$$y_{eD} = 2y_{wD} = 2y_D$$

$$z_{eD} = 2z_{wD} = h_D$$

References

[1] Gringarten A. C. and Ramey H. J. (October, 1973), "The Use of Source and Green's Functions in Solving Unsteady Flow Problems in Reservoirs". SPEJ. Vol. 13(05). pp. 285-296. SPE 3818. https://doi.org/10.2118/3818-PA

[2] Adewole E. S. (August, 2012), "Interference Tests Analyses of Horizontal and Vertical Well Combinations in a Reservoir Subject to Double-Edged Water Drive". Paper presented at the Nigeria Annual International Conference and Exhibition, Lagos, Nigeria. SPE-163033-MS. https://doi.org/10.2118/163033-MS

[3] Henry Idudje and Steve Adewole (August, 2020), "A Method of Estimating Reservoir Pressure using Drawdown Test Data" Paper presented Virtually at the SPE Nigeria Annual International Conference and Exhibition. SPE-203700-MS. https://doi.org/10.2118/203700-MS

[4] Malekzadeh D. and Tiab D. (October, 1991), "Interference Testing of Horizontal Wells." Paper presented at the SPE Annual Technical Conference and Exhibition, Dallas, Texas, U.S.A. https://doi.org/10.2118/22733-MS

[5] Emumena E., Adewole E.S. and Ojah M.G. (July, 2023), "Dimensionless Pressures and Derivative Distribution of Two Interfering Horizontal and Vertical Wells in an Infinite Acting Reservoir." Paper presented at the SPE Nigeria Annual International Conference and Exhibition, Lagos, Nigeria. SPE-217170-MS. https://doi.org/10.2118/217170-MS

[6] Ojah M.G., Adewole E.S. and Emumena E. (July, 2023), "Pressures and Pressure Derivatives of Vertical and Horizontal Wells Located Within Intersecting Sealing Fault and Constant Pressure Boundary." Paper presented at the SPE Nigeria Annual International Conference and Exhibition, Lagos, Nigeria. SPE-217103-MS. https://doi.org/10.2118/217103-MS

[7] Edobhiye O. and Adewole E.S. (August, 2014), "Effects of Both Wellbore and Reservoir Properties on Dimensionless Pressure and Dimensionless Pressure Derivative Distribution of a Horizontal Well in a Reservoir Subject to Bottom Water, Gas Cap and Single Edge Water Drive Mechanisms." Paper presented at the SPE Nigeria Annual International Conference and Exhibition, Lagos, Nigeria. SPE-172384-MS. https://doi.org/10.2118/172384-MS

[8] Ogbue M.C. (June, 2025), "Comprehensive Pressure Distribution Model for Horizontal Well in Bottom-Water Reservoir." Caritas Journal of Engineering Technology. Volume 4(01). www.caritasuniversityjournals.org

[9] Ozkan Erdal and Raghavan Rajagopal (August, 1990), "Performance of Horizontal Wells Subject to Bottom water Drive." SPE-18559-PA. Volume 5(03). https://doi.org/10.2118/18559-PA

[10] Ogbamikhumi A.V. and Adewole E.S. (January, 2020), "Pressure Behaviour of a Horizontal Well Sandwiched Between Two Parallel Sealing Faults", Nigerian Journal of Technology (NIJOTECH), Vol. 39(1), pp. 148-153. http://dx.doi.org/10.4314/njt.v39i1.16

[11] Oloro J.O, Adewole E.S. and Olafuyi O.A. (December, 2014), "Pressure Distribution of Horizontal Wells in a Layered Reservoir with Simultaneous Gas Cap and Bottom Water Drives." American Journal of Engineering Research. Vol. 3(12). pp. 41-53. www.ajer.org

[12] Oloro J.O and Adewole S.E (April, 2020), "Performance and Behavior of a Horizontal Well in Reservoir Subject to Double-Edged Water Drive." Nigerian Journal of Technology (NIJOTECH). Vol. 39(2). pp. 417 – 423. http://dx.doi.org/10.4314/njt.v39i2.11

[13] Ogbue M.C. and Adewole E.S. (September, 2013), "Theoretical Investigation of Factors Affecting Water Breakthrough Time in a Horizontal Well Subject to Bottom Water Drive." Advanced Materials Research. Trans Tech Publications, Switzerland. Volume 824(2013). pp. 394-400. https://doi.org/10.4028/www.scientific.net/AMR.824.394

[14] Oloro J. and Adewole E.S. (January, 2015), "Factors that affect pressure distribution of horizontal wells in a layered reservoir with simultaneous gas cap and bottom water drive." Journal of Petroleum and Gas Engineering. Vol. 6(1), pp. 1-9. http://www.academicjournals.org/JPGE

[15] Joshi, S.D., (September, 1990), "Horizontal well technology", Joshi Technologies International, Inc. Tulsa, Oklahoma, U.S.A.